Dorh, J., Sarua, A., Ajmal, T., Okache, J., Rega, C., Müller, G. M., & Cryan, M. (2017). Nanoantenna arrays combining enhancement and beam control for fluorescence-based sensing applications. *Applied Optics*, *56*(29), 8252-8256. https://doi.org/10.1364/AO.56.008252

Nanoantenna Arrays Combining Enhancement and Beam Control for Fluorescence Based Sensing Applications

N. Dorh[1], A. Sarua[2], T. Ajmal[3], J. Okache[3], C. Rega[4], G. M. Müller [5], and M.J. Cryan[1]

[1]Department of Electrical and Electronic Engineering, University of Bristol
[2]H. H. Wills Physics Laboratory, School of Physics, University of Bristol
[3]School of Computer Science and Technology, University of Bedfordshire
[4]ABB Limited, Gloucestershire, UK
[5]ABB Corporate Research, Baden-Dättwil, Aargau, Switzerland

Abstract:

This paper presents measured fluorescence enhancement results for ~250 x *250 element aluminium nanoantenna arrays fabricated using electron beam lithography. The arrays have been designed to use diffractive coupling to enhance and control the direction of fluorescent emission. Highly directional emission is obtained at the designed angles with beamwidths simulated to be in the range of 4-6°. Angle resolved spectroscopy measurements of dye-coated nanoantenna arrays were in good agreement with FDTD modelling. Critically, these results were obtained for near UV wavelengths (~360nm) which is relevant to a number of biosensing applications.*

Fluorescent emission from molecules is a widely used phenomenon in numerous applications ranging from bio-imaging[1] to DNA sequencing[2]. There has been much work on the fundamental science of nanoantennas to enhance and control the emission from light emitters such as fluorphores and quantum dots [3-5]. Much less work has been done to engineer the wavelength, magnitude and directionality of fluorescence emission from nanoantennas arrays for integration into real biosensing devices, especially in the UV spectrum where several important bio-indicators auto-fluoresce. This paper aims to establish benchmark performance of aluminium nanoantenna arrays using measurement scenarios that could be developed into a multiwavelength, low cost sensor platform.

Fluorescent emission coupled to nanoantenna arrays has been widely studied to understand strong and weak coupling between the molecules and array modes[4,6], however, again less emphasis is placed on the strongly directional effects obtained from large arrays. In this paper we use 2D nanoantenna arrays that are more than 100 x 100 wavelengths in area to study both enhancement and directional focusing effects. Directional effects in antenna arrays are well known in the RF domain where very large phased

array antennas are commonly used to form multiple, steerable beams [7]. In that case the electromagnetic energy is coherent and beam forming effects are to be expected. In the case of fluorescent emission, which is a spontaneous process, it is not immediately obvious that such coherent effects will occur. The coherence of the emission can be affected by whether the molecule-antenna array system is strongly or weakly coupled [8]. Literature has shown that [6,8,9] it is possible to enter the strong coupling regime when the number of emitters within the mode volume is relatively large. However, in the context of fluorescence sensing applications, the emitters tend to be spectrally broad and their concentrations relatively low, hence encouraging weak coupling. In addition, any fluorescence enhancement is contingent on the array-emitter system remaining weakly coupled [10], in this case we believe the array resonance enforces a certain level of coherence which enables beamforming effects to occur. The large number of elements used in our arrays results in very strong directional focusing effects which will be beneficial in numerous sensing applications.

Previous work in UV fluorescence enhancement [11] has shown up to 80x emission enhancement from an aluminium nanoparticle array, measured using a similar scanning photoluminescence technique to our recent work [12]. There a relatively modest 1.9x enhancement in an aluminium nanoantenna array was demonstrated for a near UV dye with a high intrinsic quantum yield (QY). This highlights a key drawback to enhancement as a figure of merit (FOM) for nanoantenna/nanoparticle efficacy, which is that the finally observed emission enhancement is a function of the intrinsic QY of the fluorophore and directivity of the array[13]. This means that, where intrinsically efficient fluorophores are used with low Purcell enhancement factors, there is still opportunity to observe an overall enhanced emission through improvements to collection due to the directivity of the array.

This paper builds on the work around diffractive coupling [8,17] to engineer the angular response of an array for applications in biosensing in the UV spectrum. The paper begins with a discussion of diffractive coupling as a method for beam control, including Finite Difference Time Domain (FDTD) modelling of the fabricated arrays. It then shows results for combined enhancement and beam control using angle resolved enhancement measurements of a near ultra-violet (NUV) dye coated nanoantenna array.

1. Emission Control by Diffractive Coupling

It can be shown that the output steering angle or emission angle (θ_{out}) for a linear array of antennas is governed by the grating equation [18] which for normal incidence is given by :

$$a = \frac{m\lambda}{\sin(\theta_{out})} \tag{1.1}$$

Where a is the array pitch, m is the diffracted order and λ is the wavelength. In our design we also want to maximise emission enhancement as well as control the emission angle and thus we must also consider individual nanoantenna resonances and array resonances, often termed surface lattice resonances where

this enhancement occurs. To account for these effects simultaneously is difficult analytically and thus here we have employed electromagnetic modelling to determine the optimum nanoantenna geometry and spacing to optimise fluorescence enhancement at given emission angles.

The other important aspect to the design is the collection optics being used. In real sensors there are numerous potential configurations that could be explored, but here we have taken a very general approach using a goniometer mounted photodetector to characterise the magnitude and angular emission from the samples. In general, in a 2D array, a uniform pitch in both directions generates a 2D diffraction pattern and as a result, spreads emission in both planes. This may not be ideal for all applications and by making the pitch sufficiently small, i.e., subwavelength, in one direction, forces diffraction to occur along a single axis, simplifying collection in the far field and further enhances emission by concentrating the fluorescence into a smaller number of diffracted orders. In principle, any emission angle over the range of 0°-90° (0° = Normal emission) can be achieved by varying the array pitch. However, steering into the range 0-30° permits additional diffraction orders to exist, which reduces the intensity of each emission lobe. It is also worth noting that when using non-goniometer collection with a single lens, emission at angles in the range 50°-90° demand a lens with a relatively high NA, upwards of 0.8, which are practically difficult. Thus, we have chosen steering angles between 30° and 50°.

1.1 Array Design

A series of aluminium nanoantenna arrays were fabricated which targeted a higher order antenna resonance near to 350 nm, since operating in the fundamental mode demands very small antennas which are very difficult to fabricate [12]. The emission was designed to be within the 30°-50° range and details of the design parameters are shown in Table 1. The arrays were fabricated using electron beam lithography and metal lift-off on a 1 mm thick fused silica substrate with a 5 nm titanium (Ti) adhesion layer. The fused silica substrate is UV transparent which is critical for any transmission based measurements. Arrays were coated by a thin layer of silicon nitride (Si_3N_4), refractive index of (n=2) [19] which acted as a passivation layer to add robustness against harsh sensing conditions within which such nanoantenna arrays could be placed.

Name	Arm length (nm)	Arm Width (nm)	Long-axis pitch/a_x (nm)	Short axis pitch/a_y (nm)	Steering Angle (°)
Array 1	158	50	544	250	40
Array 2	158	50	457	250	50

Table 1: Antenna array design table

Figure 1 shows a SEM image of array 1. In the inset, a representative measurement revealed that the element dimensions were 137 nm x 37 nm (l x w) compared to the designed dimensions of 158 nm x 50 nm. The array occupied a physical footprint of 0.1 mm x 0.1 mm and contained about 57,200 individual nanoantenna elements.

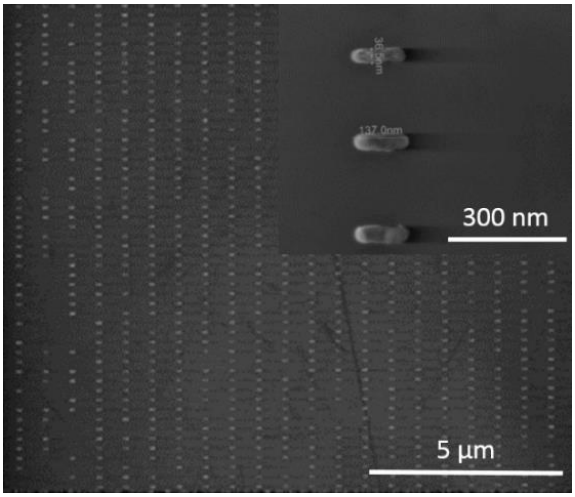

Figure 1: SEM images of nanoantenna array and in the inset a magnified view of the array elements

Figure 2 shows the FDTD model of the fabricated structures. A single aluminium nanoantenna of arm length, l, arm width, w, and arm height, h, on a substrate with , n_g=1.5, with a titanium (Ti) adhesion layer, thickness, l_a=5 nm. The entire nanoantenna was covered by a uniform passivation layer (index, n=2), thickness, l_p. The simulation was bordered by periodic boundaries in the x and y directions and PML in the z direction, this effectively represented an infinite array of horizontal pitch, a_x and vertical pitch a_y. The nanoantenna was excited by an electric dipole source (350 nm - 550 nm) positioned at the centre of the long axis, at a distance, d=15 nm from the passivation layer and polarised along the nanoantenna short axis (E_y). The data monitor was placed above the nanoantenna, in air (n= 1). Enhancement was defined as the net power through the monitor normalised to the power emitted by the source in free space.

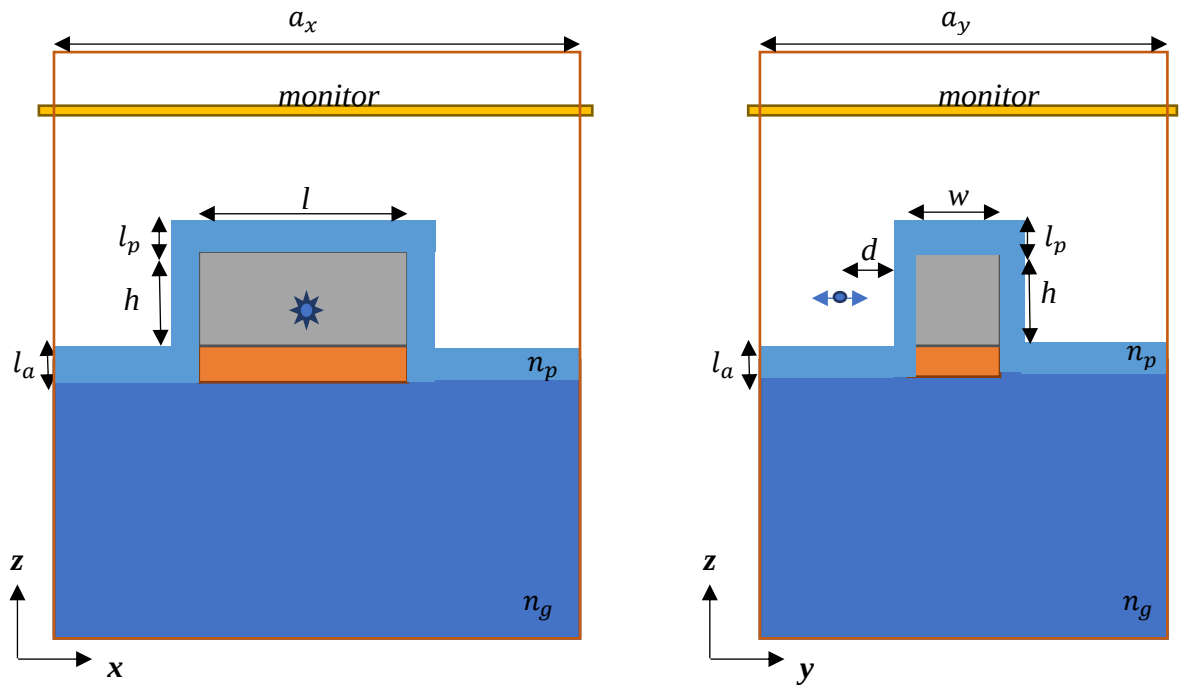

Figure 2: FDTD simulation layout; a single aluminium nanoantenna of arm length, l, arm width, w, and arm height, h, attached to substrate with RI n_g=1.5, via a titanium (Ti) adhesion layer, thickness, l_a = 5 nm. The entire nanoantenna was covered by a uniform passivation layer (index, n_p=2), thickness l_p =10 nm. The passivated structure was coated in a 50 nm layer of water, index, n_s=1.33. The simulation was bordered by periodic boundaries in the x and y directions and PML in the z direction, this effectively represented an infinite array of horizontal pitch, a_x and vertical pitch a_y=250 nm. The data monitor was placed above the layer of water, in air, RI of 1.

Figure 3(a) and (b) show the enhancement and far field emission patterns, respectively, predicted by FDTD modelling of the arrays, using both the design and fabricated dimensions. It can be seen that the shorter fabricated nanoantennas, result in blueshifted resonances compared to the design case, as might be expected. Far field projections were generated at the array resonant wavelength. In Figure 3(a) we observe higher enhancement (~1.9x) for Array 2 but lower enhancement (~1.46x) for Array 1. It is worth noting that the enhancement shown here from FDTD is effectively spatially averaged over the entire collection plane and does not fully account for the directivity and as such will impact later comparisons with measurements. Figure 3(b) shows that at resonance, based on the design dimensions; Array 1 and Array 2 are expected to steer the emission to ±47° and ±60°, respectively. However, using the representative fabricated dimensions, the emission angles for Array 1 and Array 2, become ±42° and ±52°, respectively, due to the blueshifted resonance. The FWHM beamwidth of Array 1, using representative fabricated dimensions was noticeably smaller (4°) than that of Array 2 (6°). This relationship which was also preserved with the designed dimensions; 5° for Array 1 and 8° for Array 2.

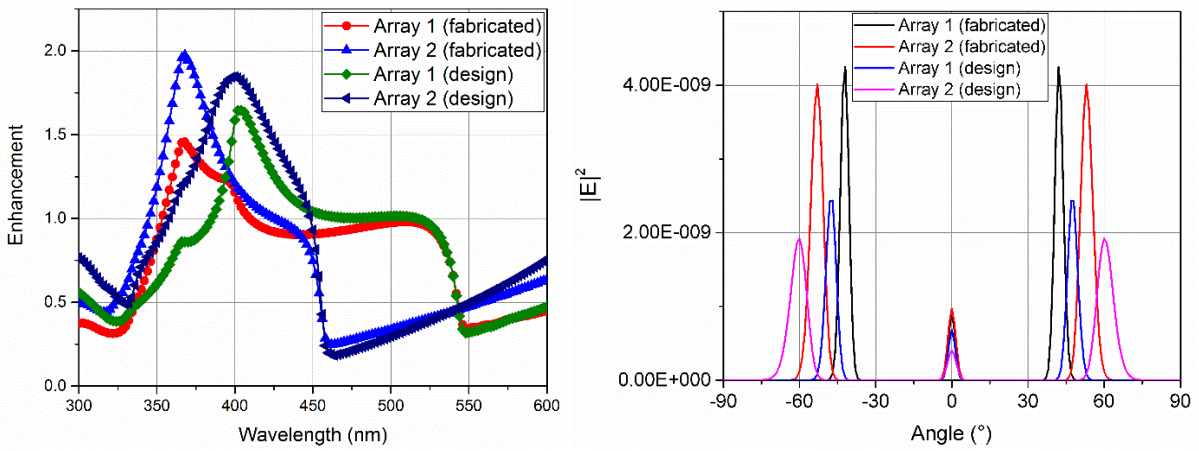

Figure 3 : (a) FDTD simulated enhancement spectra for Arrays 1 and 2 using design dimensions and representative fabricated dimensions, 137 nm x 37 nm (l x w) (b) FDTD simulated far field patterns for Array 1 ($\lambda_{fabricated} = 366\ nm, \lambda_{design} = 398nm$) and Array 2 ($\lambda_{fabricated} = 366\ nm, \lambda_{design} = 402nm$) using design and representative fabricated dimensions.

2. Angle Resolved Nanoantenna Enhancement Measurements

This section presents angle resolved photoluminescence (PL) measurements (enhancement) of Arrays 1 and 2, shown schematically in Fig 4. Each array was illuminated from below the substrate by a 325 nm LED at normal incidence with an intensity of approximately 3mW/cm^2 at the array and emission collected at varying angles. Measurements were performed over the nanoantenna array and an area of bare substrate all coated in UV dye (Exalite 392E). A 1.73 mM solution of the dye in 80:20 %vol H_2O/EtOH was prepared then deposited on the sample by drop-casting. The sample was placed on a hotplate at 70°C for 5 minutes, after which, 400 µL of the dye solution was pipetted on the sample such that the entire array area was immersed. The dye coated sample was left on the hotplate until visibly dry. Heating caused the solvent to evaporate rapidly, leaving behind a thin, uniform layer of dye. Enhancement spectra were generated by a normalisation of the intensity spectra measured from the dye over the nanoantenna array to the dye emission intensity measured over the substrate. An integration time of 5s was used to maximise collected intensity and multiple spectra averaging was used to minimise noise effects.

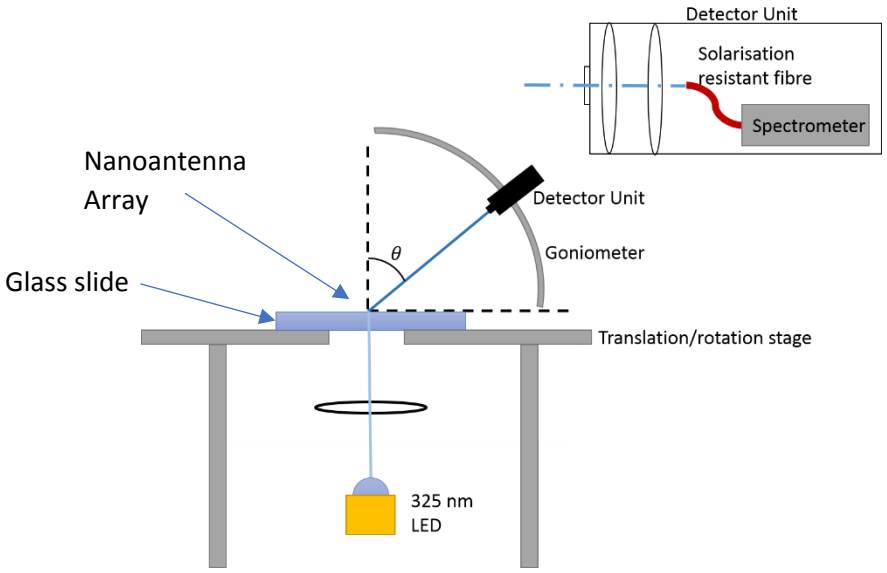

Figure 4: Goniometer based optical setup for measuring angle resolved photoluminescence measurement. The nanoantenna array was illuminated from the substrate side and emission was collected above the arrays at angles between 0° and 55°.

Figure 5 shows the enhancement spectra for Arrays 1 and 2. Figure 5(a) shows the results for Array 1 and the enhancement peak of 6x can be seen at 360 nm, which is very close to the predicted wavelength from FDTD modelling. The peak enhancement was measured at 40° collection angle again in good agreement with the FDTD modelling, it is also evident that emission was suppressed at other collection angles. Figure 5(b) shows results for Array 2 with maximum enhancement of 2.5x measured at 360 nm and at 50°, again wavelength and angle are close to that predicted by FDTD modelling. These results show that wavelength and angle can be predicted well using FDTD modelling from actual measured dimensions of the arrays, but absolute enhancement is not in good agreement. It can be seen that in general, larger enhancement was measured than predicted by FDTD. In the FDTD model, the emission was collected at all angles simultaneously and then averaged, whilst in the measurement, each angle was considered separately, which exploits the directivity of the array and more closely represents a practical sensor approach. The difference in absolute levels of enhancement is due to the very simplified nature of the FDTD model which contains only single, aligned dipoles as emitters, which due to periodic boundaries are periodically distributed. In reality there will be many more dipoles with random orientation and alignment. This model assumes identical arrays of nanoantennas, which will also not be the case. Future work will use measured SEM image data to model real nanoantenna arrays and this combined with random distributions of dipole sources will allow better estimates of absolute enhancement to be obtained.

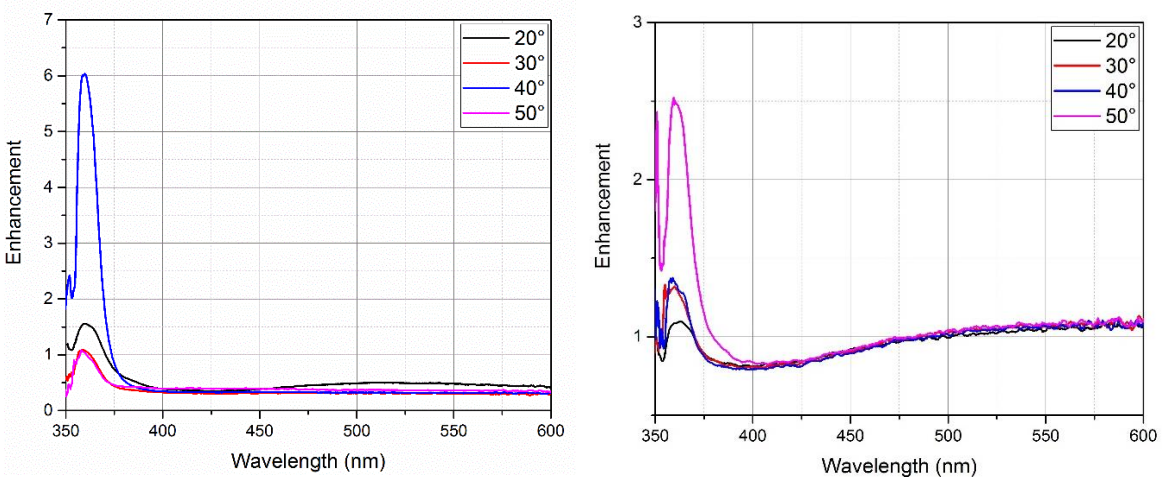

Figure 5: Enhancement Spectra at collection angles over the 20°-50° range for (a) Array 1 (b) Array 2.

At each angle, emission spectrum collected from nanoantennas was normalised to emission spectrum from nearby glass area.

3. Conclusions

This paper shows the design, fabrication and testing of aluminium nanoantenna arrays for plasmonic, fluorescence based sensing. A series of nanoantenna arrays were fabricated based on the design principles presented. Angle resolved PL measurements of Exalite 392E coated nanoantenna arrays showed up to 6x enhancement of NUV fluorescence at 360 nm; collection angles were in good agreement with FDTD modelling and the novel approach to beam steering presented in this paper. In future, low cost fabrication techniques such as nanoimprint lithography will be explored to enable the design of low cost fluorescence based sensors.

Acknowledgements: The authors acknowledge Kelvin Nanotechnology for fabrication of the nanoantenna arrays and ABB for part funding of this work.

Author Contributions: N.D. developed the FDTD model, performed the experiments and data analysis, A.S., T.A., J.O., C.R. and G.M.M. developed the experimental set-up and commented on the manuscript, M.J.C. supervised the project and commented on the manuscript.

Competing Financial Interests: The authors declare no competing financial interests.

References

1 Day, R. N. & Davidson, M. W. The fluorescent protein palette: tools for cellular imaging. *Chemical Society Reviews* **38**, 2887-2921 (2009)

2 Shendure, J. and Ji,H. , "Next-generation DNA sequencing", Nature Biotechnology Volume 26 Number 10 October 2008

3. Alberto G. Curto, Giorgio Volpe, Tim H. Taminiau, Mark P. Kreuzer, Romain Quidant, Niek F. van Hulst, Unidirectional Emission of a Quantum Dot Coupled to a Nanoantenna, Science, **20,** Vol. 329, August 2010, pp930-932

4. G. Vecchi, V. Giannini, and J. Gomez Rivas, Shaping the Fluorescent Emission by Lattice Resonances in Plasmonic Crystals of Nanoantennas, *Physical Review Letters***, 102**, 146807 (2009)

5. W. Zhang, F. Ding, W. Li, Y. Wang, J. Hu and S. Y. Chou, "Giant and uniform fluorescence enhancement over large areas using plasmonic nanodots in 3D resonant cavity nanoantenna by nanoimprinting," Nanotechnology 23, 225301 (2012)

6 Väkeväinen, A. I. *et al.* Plasmonic Surface Lattice Resonances at the Strong Coupling Regime. *Nano Letters* **14**, 1721-1727 (2013)

7 Balanis, C. A. in *Antenna Theory Analysis and Design Third Edition* 283-296 (John Wiley and Sons, 2005).

8 Shi, L. *et al.* Spatial Coherence Properties of Organic Molecules Coupled to Plasmonic Surface Lattice Resonances in the Weak and Strong Coupling Regimes. *Physical Review Letters* **112**, 153002 (2014).

9 Eizner, E., Avayu, O., Ditcovski, R. & Ellenbogen, T. Aluminum Nanoantenna Complexes for Strong Coupling between Excitons and Localized Surface Plasmons. *Nano Letters* **15**, 6215-6221 (2015).

10 Tame, M. S. *et al.* Quantum plasmonics. *Nat Phys* **9**, 329-340, (2013).

11 Jha, S. K., Mojarad, N., Agio, M., Löffler, J. F. & Ekinci, Y. Enhancement of the intrinsic fluorescence of adenine using aluminum nanoparticle arrays. *Optics Express* **23**, 24719-24729, (2015).

12 Dorh, N., Sarua, A., Stokes, J., Hueting, N. A. & Cryan, M. J. Fluorescent emission enhancement by aluminium nanoantenna arrays in the near UV. *Journal of Optics* **18**, 075008 (2016).

13 Gérard, D. & Gray, S. K. Aluminium plasmonics. *Journal of Physics D: Applied Physics* **48**, 184001 (2015).

14 DeRose, C. T. *et al.* Electronically controlled optical beam-steering by an active phased array of metallic nanoantennas. *Optics Express* **21**, 5198-5208 (2013).

15 de Ceglia, D., Vincenti, M. A. & Scalora, M. Wideband plasmonic beam steering in metal gratings. *Opt. Lett.* **37**, 271-273 (2012).

16 Adams, D. C., Thongrattanasiri, S., Ribaudo, T., Podolskiy, V. A. & Wasserman, D. Plasmonic mid-infrared beam steering. *Applied Physics Letters* **96**, 201112 (2010).

17 Ng, B. *et al.* Lattice resonances in antenna arrays for liquid sensing in the terahertz regime. *Optics Express* **19**, 14653-14661 (2011).

18 Wise, S. *et al.* Phase Effects in the Diffraction of Light: Beyond the Grating Equation. *Physical Review Letters* **95**, 013901 (2005).

19 Philipp, H. R. Optical Properties of Silicon Nitride. *Journal of The Electrochemical Society* **120**, 295-300 (1973).